Hindawi Publishing Corporation
VLSI Design
Volume 2008, Article ID 437879, 9 pages
doi:10.1155/2008/437879

Research Article

A Dependable Microelectronic Peptide Synthesizer Using Electrode Data

H. G. Kerkhoff,[1] X. Zhang,[1] F. Mailly,[2] P. Nouet,[2] H. Liu,[3] and A. Richardson[3]

[1] *Testable Design and Test of Integrated Systems Group, Centre of Telematics and Information Technology (CTIT), 7500AE Enschede, The Netherlands*
[2] *Microelectronics Laboratory (LIRMM), University of Montpellier, 34392 Montpellier Cedex 5, France*
[3] *Centre for Microsystems Engineering, University of Lancaster (ULAN), Lancaster LA1 4YW, UK*

Correspondence should be addressed to H. G. Kerkhoff, h.g.kerkhoff@utwente.nl

Received 31 October 2007; Revised 28 February 2008; Accepted 23 May 2008

Recommended by José Machado da Silva

The research in the area of microelectronic fluidic devices for biomedical applications is rapidly growing. As faults in these devices can have serious personal implications, a system is presented which includes fault tolerance with respect to the synthesized biomaterials (peptides). It can employ presence and purity detection of peptide droplets via current (charge) tests of control electrodes or impedance (phase) measurements using direct sensing electrodes near the peptide collector area. The commercial multielectrode array performs better in pure and impure detection of peptides in impedance and phase. Our two-electrode X-MEF case shows slightly poorer results. In both cases the phase is the best choice for contents detection. If there are presence or purity problems, the location is marked, and repeated peptide synthesis at another collector site is initiated.

1. INTRODUCTION

There is a rapid increase in with the complex control and massive signal processing nowadays available in advanced CMOS technology [1]. This development is especially of importance in life-science applications. However, in these applications, usually strict regulations are applied in terms of patient safety and the quality of materials used.

In a previous paper, we have suggested the implementation of a new droplet-based peptide synthesizer for point-of-care diagnostics using a new advanced heterogeneous technology, combining automotive SoC and fluidics technology [2]. As defects in these devices can have serious personal implications, like an incorrect initial diagnosis of cancer or virus, a system is presented in this paper which includes fault tolerance with respect to the quality of synthesized (peptide) biomaterials.

Our approach employs new presence and purity detection of peptide droplets via current or impedance measurements using either *control* or *direct sensing* electrodes near the peptide collector area. In the case of droplet presence or purity problems, the location is marked in the embedded RAM-based database, and repeated synthesis at the same or another site is initiated.

2. PEPTIDE SYNTHESIS

Our previously presented microelectronic fluidic (MEF) device [2] is able to synthesize many peptides via the conventional Fmoc method, but at a *micro*scale. This new device is fully software programmable, via a dedicated on-chip processor tailored for massive parallel fluidic operations and calculations.

As a demonstrator, we have studied a peptide consisting of nine amino acid elements (9-chain).

AMLDLLKSV

This particular antigenic peptide is being used for the detection of soft tissue sarcoma (STS), a form of cancer [3].

Because in the normal process of peptide synthesis some amino acids may be less efficient in peptide coupling reactions (between 5% and maximum 20%), we have compared

the previous "pure" peptide with the following *potential side-product, the* 8-mer peptide.

AMDLLKSV

This 8-mer potential impurity may be considered as an altered peptide ligand (APL) [4], a nonimmunogenic modification of the original antigenic peptide. The *immune response* of a T-cell (category of white blood cells in blood) is crucial for cancer detection as it recognizes the presented antigenic peptide. For details is referred to the general biomedical literature. An APL will only rarely cause this immune response and together with the requirement of sufficient volume, it is hence unlikely to result in a false alarm with regard to cancer detection.

In the normal case, peptide binding and cancer cell detection takes place in two steps: first, the MHC tetramers (set of molecules displayed on cell surfaces that are responsible for antigen presentation) have to be charged with peptide, and after a sufficient amount of MHC tetramers have been loaded with *antigenic* peptide, they will interact with the T-cell receptor of cancer cell specific T-cells indicating the presence of cancer cells that present this particular antigen.

As a result, it is not important to determine *which* APLs are involved (test all kind of chain permutations) or how much (volume percentage), but rather take care that sufficient (10 nmol) pure peptides are present to guarantee correct immune response detection. Any deviation exceeding the pure peptide measurement error (<1%) will result in the setting of a flag in our software. This flag will start up our fault tolerance procedure as discussed in Section 6. Subsequent proper action can be choosing another peptide collector site and start afresh, or enhancing the current site with more pure peptides and remeasure.

3. PEPTIDE PRESENCE AND PURITY TESTS VIA CONTROL AND DIRECT SENSING ELECTRODE MEASUREMENTS

It has been shown in the past, that there is a direct relationship between the degree of binding of amino acids in a peptide using solid-phase synthesis and the peptide conductivity [5]. Hence, one approach to detect the purity of a peptide is to measure the *conductivity* of the fluid containing the peptide by using *direct sensing* electrodes. The latter means there is a direct contact between the electrodes and the biofluid. In [5], the electronics for measuring this *conductance* have been suggested; it uses discrete operational amplifiers and passive components to achieve its goal.

As an alternative approach, the change in dielectric value of a pure/impure peptide droplet could be used for this purpose [6, 7]. This employs capacitive *control* electrodes (not in direct contact with the fluid) and further requires RF sources. However, this would result in a complex implementation on a chip.

We will discuss our two new test methods: one using (capacitive) *control* electrodes and transient current sensors as test infrastructure, while in the other approach, *direct sensing* electrodes measuring the phase at low frequencies is being used. Together, they form a powerful evaluation set in order to obtain a dependable MEF device.

4. TESTS BASED ON CONTROL ELECTRODE AND DIRECT SENSING ELECTRODE INFRASTRUCTURES

At the end of the peptide synthesis cycle, it has been shown to be of key importance to be able to detect the presence and purity of the produced peptides on the MEF top substrate [2]. Instead of the traditional chemical method in *macro*synthesis, we intended to use some electrical way for on-chip peptide presence and purity detection. Two methods are proposed in this paper: using the droplet *control* electrodes or the *direct sensing* electrodes; they can also be used simultaneously.

Both methods have been evaluated by actual measurements on our MEF, and for direct sensing, our MEF device and a commercial multielectrode array (MEA) device [8, 9] have been used for comparison. The base solution for dissolving the peptides was 0.1% TFA. This is Triflouroacetic acid, usually employed for peptide cleavage at the last step of peptide synthesis. The droplets containing these target peptides for the pure and impure cases have a concentration of 0.5 mmol/L.

During the measurements, three droplet cases have been considered. They are 0.1% pure TFA, 0.1% TFA with pure peptide, and 0.1% TFA with impure peptide; hence only the solution contents changes, from pure TFA to a TFA mixture with peptide. The measurement methods and results will be separately discussed for both types of electrodes.

4.1. Control electrode measurements

Our microfluidic X-MEF chip, wire-bonded on a PCB which has been used in the test experiments, is shown in Figure 1(a) (top right).

The top left of the figure shows both the control (serrated edged rectangles) and direct sensing electrodes (two white dots) in that chip. They are accessible from the interface ports on the PCB.

The bottom of Figure 1(a) shows the second object of our measurements, being the multielectrode structure of a commercially available MEA device [8, 9].

This is a commercial design and not directly linked to our X-MEF design. However, it can serve to show if it is worthwhile to extend our *two*-direct sensing electrodes to *many* electrodes for the sake of increased measurement sensitivity. Figure 1(b) shows a cross-section of the combined fluidic SoC chip [2]. Basically, the fluidic part is built on top of an SoC using our proven interconnect technology. The SoC contains all (driver and measurement) electronics and digital signal processing (DSP) hardware. The control electrodes are made of Platinum, while the direct sensing electrodes use TiN. A photomicrograph of the layout of the fluidic part in the right top of Figure 1(a) shows two-droplet input channels (left & right), which merge in a third channel forming a cross. At the bottom end of this third channel, the green arrow indicates the location of the two-direct sensing

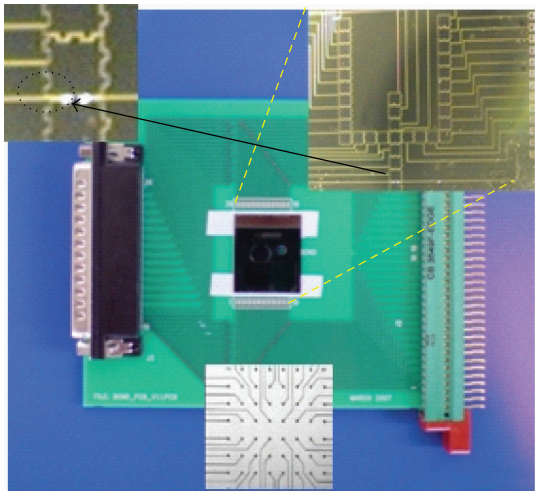

(a) Our X-MEF chip and PCB (top), and the commercially available MEA (bottom)

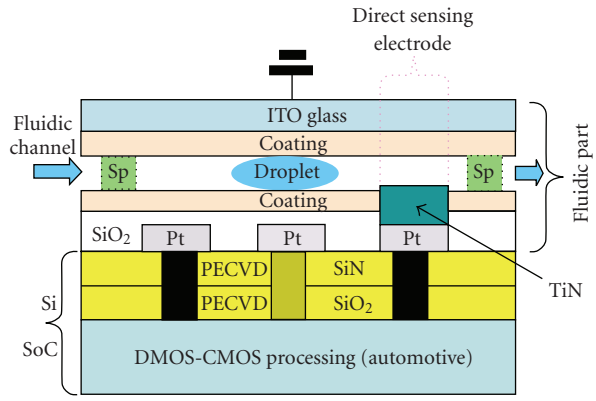

(b) Cross-section of the combined fluidic SoC chip

FIGURE 1: experimental PCB including our fluidic chip (X-MEF) for tests on direct sensing electrodes and control electrodes [1, 2].

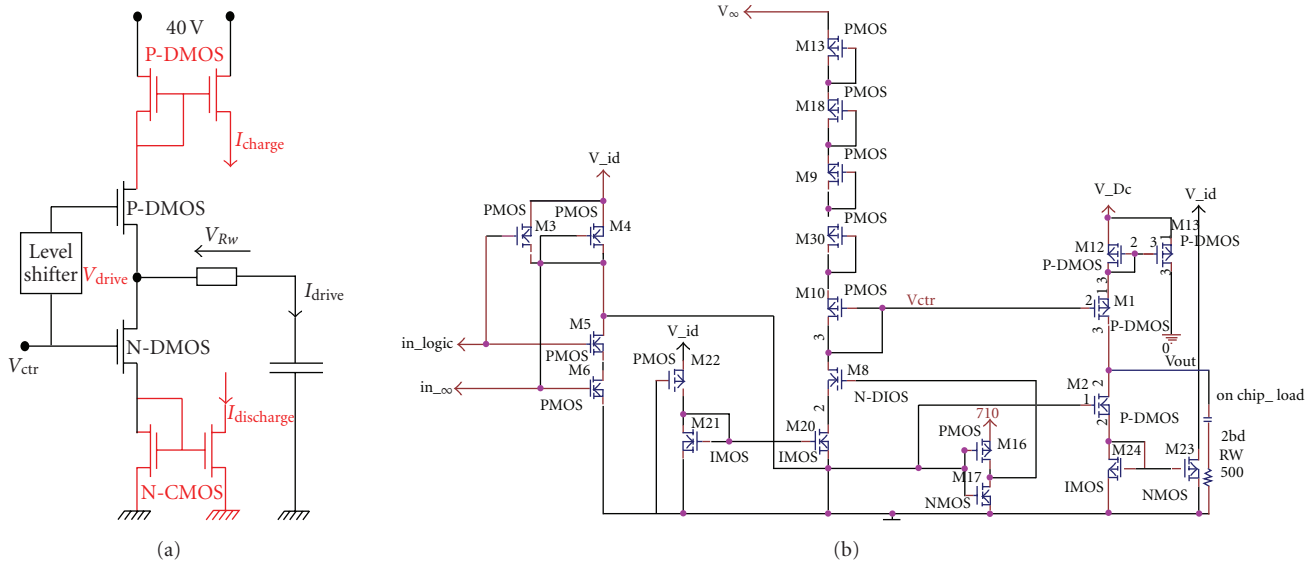

FIGURE 2: The DMOS-CMOS interface circuit schematics. (a) Basic principle of the DMOS-CMOS high-voltage driver. Red parts indicate the additional test hardware required for the peptide presence and purity detection. The capacitor represents the control electrode impedance. (b) Complete implemented DMOS-CMOS interface circuit scheme.

electrodes of which a detailed view is seen on the top left of Figure 1(a).

For droplet movement control, a DMOS-CMOS level shifter circuit was designed to "amplify" the digital control signals from a 3.3 V SoC control system into a higher voltage (40 V–80 V). This circuit is suitable to drive the control electrodes on the device and thus facilitate the transport and other operations of droplets. Besides their usage for transporting the droplets, the control electrodes can also be *reused* for detection purposes: capacitive sensing for the presence and contents of droplets.

Figure 2(a) shows the principle of the double-diffused MOS (DMOS) high-voltage driver used for droplet motion. The voltage V_{drive} is controlled by the control voltage V_{ctr}. When V_{drive} is applied, the electrode capacitance is charged through the P-DMOS transistor. It is subsequently discharged through the N-DMOS transistor when V_{drive} is switched off. The charge (or discharge) current I_{drive} is directly linked to the capacitance by

$$Q = C \cdot V_{\text{drive}} = \int I_{\text{drive}} \cdot dt = \int (V_{Rw}/Rw) \cdot dt, \qquad (1)$$

where Rw denotes the wire and itanium tin oxide (ITO) glass resistance from the top ITO plate (peptide collector site) to ground (Figure 1(b)) [2]. Its value is around 350 Ω. The transient voltage V_{Rw} across Rw was measured and recorded

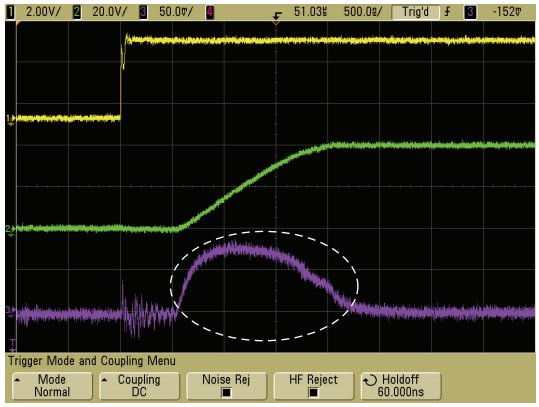

Figure 3: Actual transient measurement: rising edge control voltage V_{ctr} (yellow, 2 V per grid), V_{drive} (green, 20 V per grid), and V_{Rw} (purple, 50 mV per grid) for droplet with pure peptide.

using an oscilloscope in order to deduce the transient of current along the output path of the DMOS driver. The complete schematic of the DMOS-CMOS circuit, which we designed and implemented, is shown in Figure 2(b).

Therefore, our proposed architecture for presence and purity detection is based on the monitoring of the *(dis)charging current*. The latter can be duplicated by using a P-DMOS current mirror, while the discharge equivalent may be copied by an N-CMOS current mirror (red parts in Figure 2(a)).

The discharge current has been converted into a voltage via a transimpedance circuit and subsequently integrated; this result is then converted into a digital word via an 8-bit ADC. These parts have currently been implemented in a field-programmable analog array (FPAA). As for the purity test by impedance measurements later, the digital output value is then compared to the typical values of the pure peptides stored in an SRAM in the SoC.

Figure 3 shows part of the measurement results based on using the control electrodes in the case of only pure peptide droplets, according to Figure 2(a). Similar measurements were carried out with only the impure peptide droplets. These measurements of the transient voltage V_{Rw} have shown indeed that the charge current is linked to the purity of the peptides. Moreover, as the area under the purple curve is different in the case of pure and impure peptides, one can state that the electrode capacitance increases with the peptide purity.

Table 1 provides the results of using the structure in Figure 2 for purity detection, based on measurement data similar to Figure 3. The time interval (X-axis) was about 3 microseconds, and the charge through the top and bottom mirror parts of the driver circuit (Figure 2) at the rising and falling edge of the control voltage was compared for different droplet situations.

Table 1 shows that the top mirror under a rising edge of the control voltage resulted in the largest changes between pure and impure peptides. The results were reproducible and well within 1% tolerance. Presence detection (no solution) is very simple to implement.

Table 1: Percentage differences in measured values compared to pure peptide solution for top mirror (m12, m13) and bottom mirror (m23, m24) for rising and falling edge of the control voltage.

Condition	Top mirror, rising edge	Bottom mirror, falling edge
Pure peptide	0	0
Impure peptide	5,5%	4,1%
TFA solution	8,9%	7,0%
No solution	18,1%	14,3%

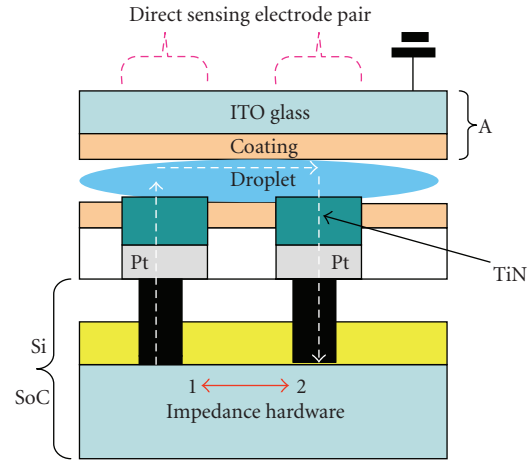

Figure 4: The direct sensing electrode pair infrastructure. The impedance is measured between nodes 1 and 2.

Hence our new structure based on control electrodes and transient current measurements could be used for our purposes. In the remaining part of this paper, we will investigate the merits of *direct sensing* electrodes in this respect.

4.2. *Direct sensing electrode measurements (X-MEF)*

Our second approach for presence and purity detection uses the direct sensor electrode *pair* of the X-MEF (Figure 1). A cross-section of this pair is presented in Figure 4; notice that the fluidic droplet flow, in contrast to Figure 1(b), is in this case perpendicular to the drawing. Impedance measurements have been carried out between the nodes 1 and 2 (Figure 4).

One can model this direct sensing electrode infrastructure as two-interfacial capacitances (C_{EDL}) in series with a solution resistance (R_{SOL}) and a solution capacitance (C_{SOL}) as shown in Figure 5. C_{EDL} represents the electrical double layer in the electrode-electrolyte interface dominating the interfacial impedance; for more details on direct sensing electrode modelling, especially for the MEA, [9] is useful.

The direct sensing electrode tests used a standard impedance setup. The test infrastructure consists of two Pt/TiN electrodes with dimensions of $50 \times 50\,\mu$m, making direct contact with an on-top droplet. Since the sensing

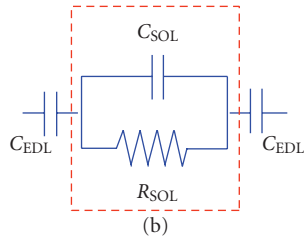

Figure 5: Simple component model of direct sensing electrode pair.

electrodes have direct contact with the droplet, impedance spectroscopy theories using the X-MEF can be applied [6, 7]. Hence we carried out impedance measurements instead of the (dis)charging method as discussed previously.

We used a Wayne Kerr precision impedance analyzer 6500 to analyze the impedance variation of the droplets containing different materials; the sweep frequency range was set from 1 kHz to 50 MHz.

In Figure 6(a), the actual measurement results are shown in case of a *pure* peptide. The top plot shows the impedance (10 Ω–1 MΩ scale), the lower plot depicts the phase (−80 deg–+40 deg scale) versus the frequency (1 kHz–50 MHz). Figure 6(b) presents the results of the impedance in all droplet content cases versus the frequency. If no fluid (e.g., peptide droplet) is present at the direct sensing electrode pair location, an (expected) pure capacitive behavior was observed and hence peptide droplet presence detection is extremely simple. A detailed graph in the case of droplet purity differences derived from Figure 6(b) is shown in Figure 6(c). Note that the frequency range was chosen here on the basis of the value of the phase most close to zero degrees because in that case the *droplet solution* content (Figure 5) is dominating other effects. At a frequency of 33 kHz, only a 1% impedance variation was observed between pure and impure peptides. This is in the range of the measurement tolerance (<1%) and can therefore not be used for purity detection.

Figures 6(d) and 6(e) show the same approach, but now in the case of the phase. The largest variations (17%, at 33 kHz) are found via the phase as compared to the previous impedance test with regard to purity/impurity detection.

This is therefore the preferred approach for impurity tests. The results were reproducible and well within acceptable tolerances (<1%) and hence usable for purity detection using the X-MEF direct sensing method.

An alternative multielectrode layout (now only *two* electrodes are used, Figure 1(a) top (left) is expected to enhance the measurement variations and accuracy even more; it will be investigated in future research work.

4.3. Direct sensing electrode measurements (MEA)

As a first step in that direction, we have also carried out similar tests with regard to a direct sensing electrode infrastructure of the multielectrode array (MEA) which is commercially available [8, 9].

This electrode infrastructure is shown in Figure 1(a) at the bottom. Although our tests are currently confined to two electrodes only, the multielectrode potential is clearly available.

The X-MEF cross-section in Figure 4 is easily converted into a two-electrode MEA infrastructure, by removing both the Si-SoC and A part.

Similar measurements using the same content *fluids* (not droplets!) were carried out on a *direct sensing* electrode *pair* in the MEA [8] (see Figure 1, bottom). The modelling of this infrastructure has been discussed in [9]. This experiment was carried out in order to see whether any similarities exist between the MEA and X-MEF, and in longer term, whether more electrode pairs could provide more reliable data on presence and contents of fluids/droplets.

Although the devices differ in amount of fluid used, distance between electrodes (layout) and used materials and electronics, trends should be similar.

Figure 7(a) presents the measurement screenshot of impedance and phase in the case of a pure peptide *fluid* over a large frequency range. Figure 7(b) shows the measurements of the impedance for all possible fluid cases. It shows that the presence detection for a fluid (e.g., peptide) is very easy. A zoomed in representation of the impedance in Figure 7(c) reveals that the variation in pure and impure peptide contents is around 5.3% in the area of interest. Figure 7(d) shows the phase versus frequency for all fluid contents cases which indicates also a very simple detection of fluid presence. Figure 7(e) presents a zoomed in version of Figure 7(d); calculations show a variation of 20% in phase at 29 kHz between a pure and impure peptide fluid. Clearly, also in the case of the MEA, the largest variations are found via the phase with regard to purity/impurity detection. The results were reproducible and the measurement tolerances less than 1%.

When comparing the data in detail of Figures 6 and 7 of the XMEF and MEA, respectively, one can draw the following conclusions: the MEA performs better in pure and impure detection of peptides in impedance and phase, and the phase is the best parameter to be used. The X-MEF case shows somewhat poorer results, but also the phase is the best choice for contents detection. The difference in test frequencies and absolute values of impedance and phase stems from the difference in structure between the X-MEF and MEA.

In the next two paragraphs will be elaborated how the previous measurements can be used to increase the dependability of the peptide synthesis process. First, the construction and location (collector) of the sensors are discussed in detail. After that, the results of these measurements are used to start up a new peptide synthesis sequence. This is implemented in software.

5. THE PEPTIDE COLLECTOR SITE

In a previous paper [2], several electrode configurations have been suggested for monitoring droplet presence and contents. The situation in our case is different, as the purity of the peptide has to be determined at a collector site. This collector site consists of a deep-etched trench in the top ITO

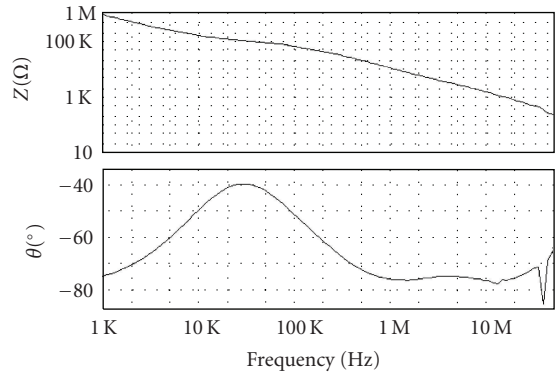

(a) X-MEF direct-sensing electrode pair measurement in the case of a pure peptide droplet. Impedance and phase versus frequency

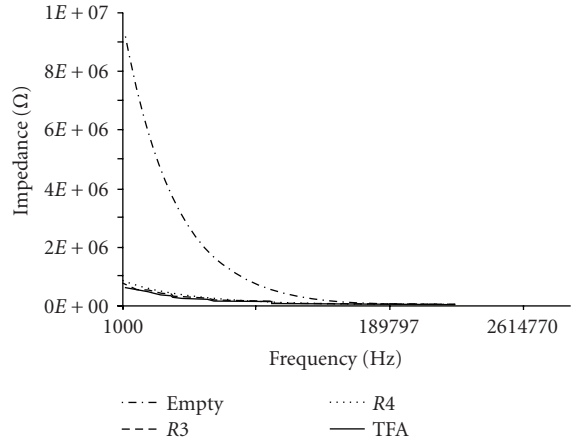

(b) Measured X-MEF direct-sensing electrode pair impedance in the case of droplet absence (empty), TFA, pure (R3), and impure (R4) peptide droplets

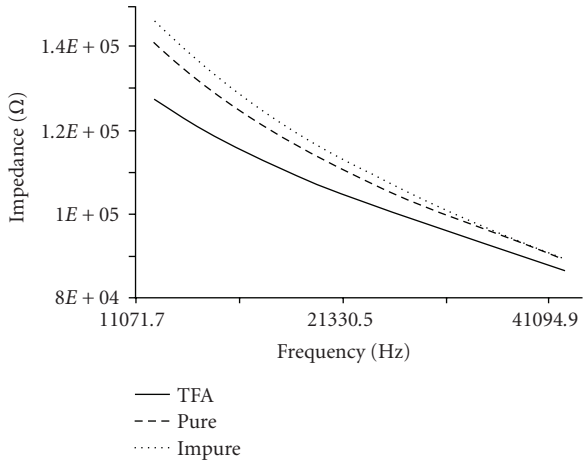

(c) Previous measurement zoomed in for the last three droplet cases under phase condition

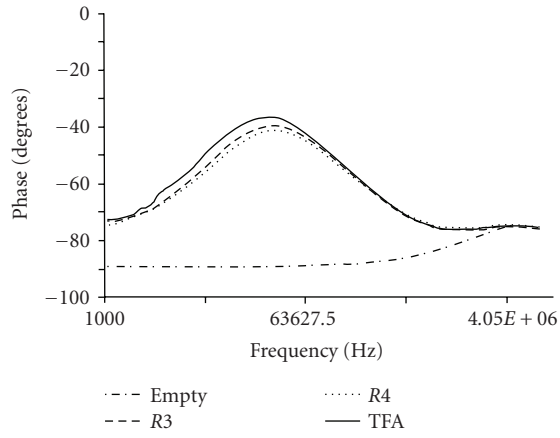

(d) Measurement of X-MEF direct sensing electrode pair phase in the case of droplet absence, TFA, pure (R3) and impure (R4) peptide droplets

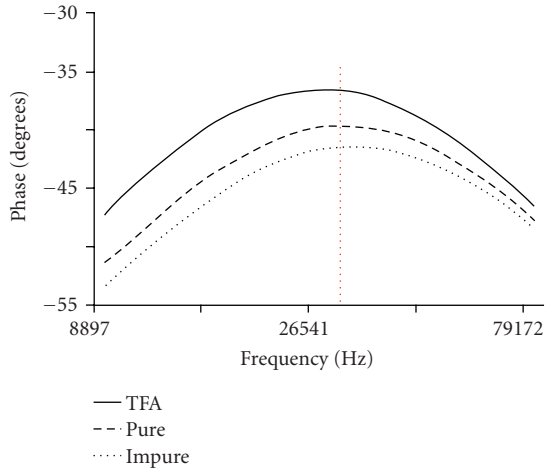

(e) Previous measurement zoomed in for the last three droplet cases under phase condition

Figure 6: X-MEF measurement results from the direct sensing electrode pair infrastructure.

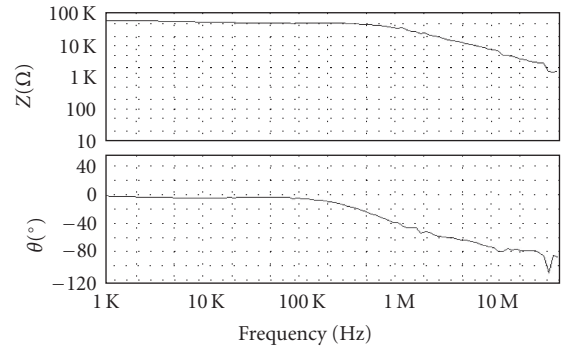

(a) MEA direct sensing electrode pair (62-63) measurement in the case of a pure peptide fluid. Impedance (10 Ω–100 kΩ scale) and phase (−120 deg–40 deg scale) versus frequency (1 kHz–50 MHz scale)

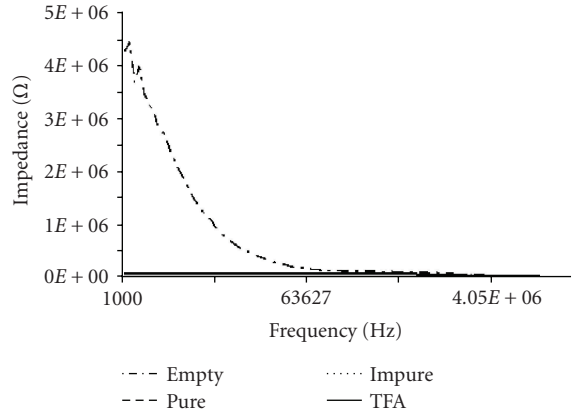

(b) Measured MEA direct sensing electrode pair impedance in the case of droplet absence (empty), TFA, pure, and impure peptide fluids (1 kHz–407 kHz frequency range)

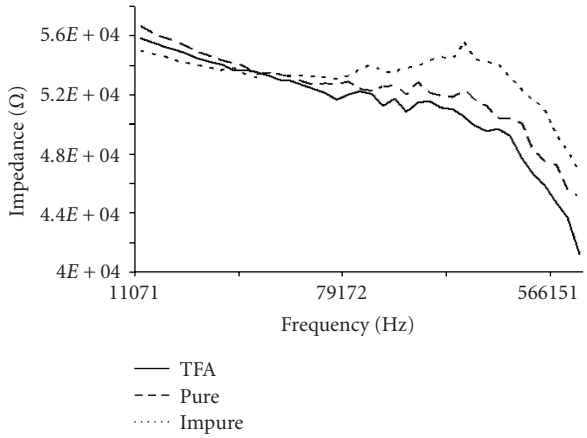

(c) Previous measurements zoomed in for the last three droplet cases in the 11 kHz–70 kHz range

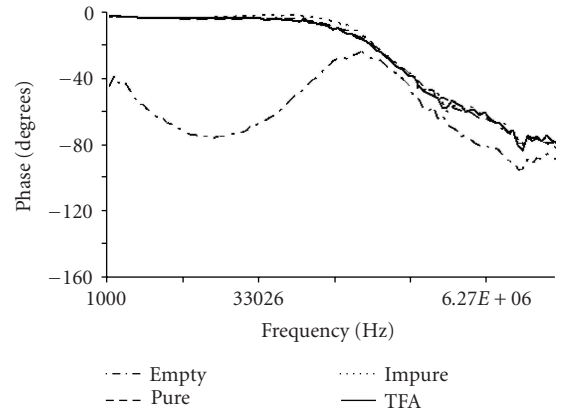

(d) MEA direct sensing electrode pair phase measurements in the case of droplet absence, TFA, pure, and impure peptide droplets (1 kHz–1.2 MHz frequency range)

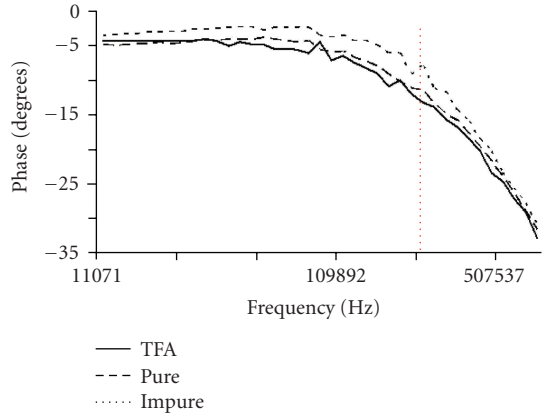

(e) Previous phase measurements zoomed in for the last three droplet cases in the 11 kHz–70 kHz frequency range

Figure 7: MEA direct sensing electrode pair (electrode # 62 and # 63) measurements of impedance and phase.

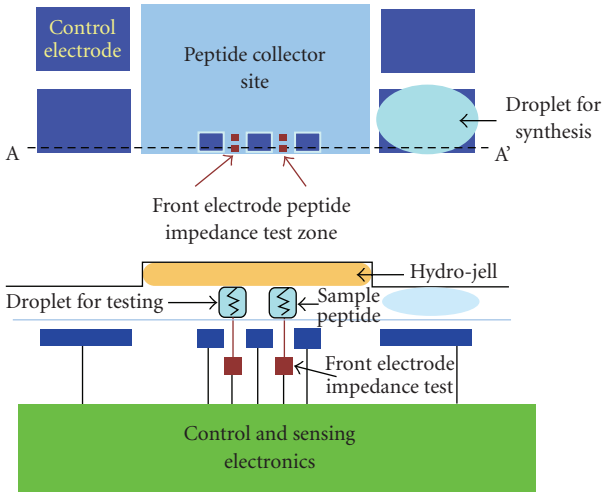

FIGURE 8: The direct sensing electrodes at the peptide collector site. Usage is made of special test droplets for purity detection.

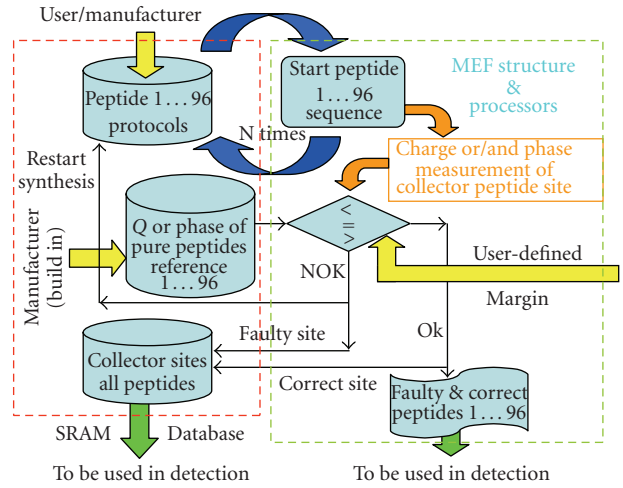

FIGURE 9: The handling of pure and impure peptide collector sites, employing the previous measurement techniques.

glass, and filled with a porous hydro gel. This approach is required to obtain sufficient peptide material for accurate cancer cell detection. Although a single pair of direct sensing electrodes can be used (shown in Figure 8, and used in the previous tests), also other, more complex options are open, as for example, like the ones used in an MEA as employed by QinetiQ [8]. Our current approach is depicted in Figure 8. The lower figure is the cross-section of A-A'.

Our system uses a special test droplet, which is smaller in dimensions than the ones during synthesis and consists of an acid solution, which cuts part of the peptide from the collector site. The droplet now contains the peptide; for enhancing the sensitivity three measurements are taken subsequently. The previously discussed tests at the chosen frequency (e.g., f_{lo} = 33 kHz) can be carried out by for instance a bridge structure [9].

6. FAULT TOLERANT PEPTIDE SYNTHESIS

The electronics in the SoC implementing the previous measurement system will send the droplet presence and contents information (based on control-electrode transient current or/and direct sensing electrode(s) phase) in digital form to our on-chip general processor (ARM), fluidic-specific coprocessor, and embedded RAM (Figure 9). Here, it will be decided if the deviation in measured peptide purity (or in worst-case absence) jeopardizes the correct (cancer or virus) detection. If so, the collector site is flagged and its location stored in the database. The digital information in terms of charge or phase of a specific pure peptide can be loaded in advance by the manufacturer, together with the measurement tolerance band and required boundary conditions (e.g., the frequency).

After flagging, a new round for synthesis will be initiated by the processor of that peptide, at either the *same* location or another site. Which decision is made depends on the measurement results. If no presence of peptides has been detected, probably the original collector site is unreachable or faulty and hence another free site will be allocated. If a large deviation (>10% margin, but software adjustable) from the pure peptide data has been detected, it is also decided to go to another site as the site can only contain a limited volume of fluids and a certain minimum is required for immune response. Only if a slight deviation (<5% margin, but software adjustable) is noticed from pure peptides, the same site will be used to add additional pure peptide via synthesis. This location information is also automatically stored and this means that a direct link exists between the original collector site, and the correct one; this is essential in the next optical step for cancer detection [10]. The simplified procedure is illustrated in Figure 9.

The user (or manufacturer) indicates which peptides have to be synthesized. These are specific to the cancer cells to be potentially detected. Currently, one can maximally provide 96 peptides on a single substrate. Multiple peptides are synthesized in parallel. By using our approach, a *dependable* MEF system results, which is a prerequisite for the application in a biomedical environment. All software has been written in C++ and runs on the on-board processor.

7. CONCLUSIONS

In this paper, two new test techniques have been investigated to determine the presence and purity of synthesized peptide droplets in our MEF and a commercial MEA via measuring the charge and phase of the biomaterial. Use is made of either direct sensing electrode pairs or control electrodes. It has been shown that detection is possible in both cases. The result is used to mark collector sites of insufficient pure peptides which could obscure cancer detection, and relate them to (a) pure site(s). In this way, the quality of cancer detection in this type of device is significantly increased, resulting in a *dependable* point-of-care device. Multielectrodes for sensing and additional DSP are seen as a possibility to further enhance the quality of measurements. A very strong point of our SoC-MEF approach is that the system is scalable in the

future to offer fully automatic dependable diagnosis in life sciences by on-the-fly specific peptide generation depending on previous diagnostic measurement results of the sample.

ACKNOWLEDGMENTS

The authors want to acknowledge H. Ovaa and B. Rodenco of the Dutch Cancer Institute for providing the special peptides for our experiments and for the contributions on biochemical issues. This research has been partly supported by the European FP6 NoE PATENT-DfMM, in the framework of the flagship project "BioDrop." Finally, support was provided by J. Li from the MESA+ BIOS group with regard to the first initial impedance measurements on peptides in MEFs.

REFERENCES

[1] H. G. Kerkhoff, "Testing microelectronic biofluidic systems," *IEEE Design & Test of Computers*, vol. 24, no. 1, pp. 72–82, 2007.

[2] H. G. Kerkhoff and X. Zhang, "Fault simulation of heterogeneous integrated biological systems," in *Proceedings of the 12th IEEE International Mixed Signals Testing Workshop (IMSTW '06)*, pp. 129–134, Edinburgh, UK, June 2006.

[3] N. H. Segal, N. E. Blachere, J. A. Guevara-Patiño, et al., "Identification of cancer-testis genes expressed by melanoma and soft tissue sarcoma using bioinformatics," *Cancer Immunity*, vol. 5, p. 2, 2005.

[4] G. J. Kersh and P. M. Allen, "Structural basis for T-cell recognition of altered peptide ligands: a simple T-cell receptor can productively recognize a large continuum of related ligands," *Journal of Experimental Medicine*, vol. 184, no. 4, pp. 1259–1268, 1996.

[5] BioTech Instruments Ltd, UK, Patent PCT/6B90/00422, 1990.

[6] H. G. L. Coster, T. C. Chilcott, and A. C. F. Coster, "Impedance spectroscopy of interfaces, membranes and ultrastructures," *Bioelectrochemistry and Bioenergetics*, vol. 40, no. 2, pp. 79–98, 1996.

[7] S. Gawad, K. Cheung, U. Seger, A. Bertsch, and P. Renaud, "Dielectric spectroscopy in a micromachined flow cytometer: theoretical and practical considerations," *Lab on a Chip*, vol. 4, no. 3, pp. 241–251, 2004.

[8] http://www.patent-dfmm.org/biodrop/presentations/QinetiQ%0BioDropPresentation.pdf.

[9] H. Liu, N. Dumas, and A. Richardson, "Self-testing of microelectrode array implemented as a bio-sensor," in *Proceedings of the 13th IEEE International Mixed Signals Testing Workshop (IMSTW '07)*, pp. 166–170, Póvoa de Varzim, Portugal, June 2007.

[10] A. Ymeti, J. S. Kanger, J. Greve, et al., "Integration of microfluidics with a four-channel integrated optical Young interferometer immunosensor," *Biosensors & Bioelectronics*, vol. 20, no. 7, pp. 1417–1421, 2005.